The Acraman asteroid impact, South Australia: magnitude and implications for the late Vendian environment

GEORGE E. WILLIAMS[1] & MALCOLM W. WALLACE[2]

[1]*Geology and Geophysics, University of Adelaide, SA 5005, Australia (e-mail: george.williams@adelaide.edu.au)*
[2]*School of Earth Sciences, University of Melbourne, Victoria 3010, Australia*

Abstract: Acraman, located in the 1.59 Ga Gawler Range Volcanics on the Gawler Craton, South Australia, is a complex impact structure that is now eroded $\geqslant 2.5$ km below the original crater floor. The geology, geomorphology, apatite fission-track geochronology, and geophysical signature of Acraman suggest that the original crater comprised highly disturbed rocks of a central uplift, a transient cavity up to c. 40 km in diameter, and a possible final structural rim at 85–90 km diameter. Radial unfolded distance from the centre of Acraman, versus decompacted thickness for the Acraman ejecta horizon identified in late Vendian (c. 580 Ma) mudstone in the Adelaide fold belt, Torrens Hinge Zone and Officer Basin up to 540 km from the impact site, accords with a transient cavity diameter of c. 40 km. The estimated impact energy for Acraman exceeds the threshold of 10^6 Mt set by earlier workers for global catastrophe. The impact occurred at a low palaeolatitude (c. 12.5°) and probably perturbed the atmosphere in both the northern and southern hemispheres. The Acraman impact probably caused a severe perturbation of the late Vendian environment, a finding consistent with independent data from the Vendian palynology of Australia that the Acraman impact induced a biotic crisis.

Keywords: Vendian, impact craters, ejecta, palaeoenvironment.

In the two decades since Alvarez *et al*. (1980) presented the then highly controversial hypothesis that the Cretaceous–Tertiary (K–T) mass extinction resulted from a major impact, much attention has been directed to assessing the environmental perturbations and hazards caused by the impact of asteroids and comets with the Earth (Chapman & Morrison 1994; Gehrels 1994; Toon *et al*. 1997). Although the effects of major impacts have been investigated as possible causes of Phanerozoic extinction events (e.g. Raup 1992; Koeberl & MacLeod 2002), little work has been directed to ascertaining the environmental perturbations caused by Precambrian impacts and their possible influence on the biological record. Hence the conclusion of Grey (2001) and Grey *et al*. (2003), based on the Vendian acritarch record in Australia, that the late Vendian Acraman impact in South Australia may have induced a biotic crisis is important in focusing attention on the possible effects of major impacts on Precambrian evolution.

Acraman (Fig. 1) is a complex impact structure (see Melosh 1989, p. 130) that is now eroded several kilometres below the original crater floor (Williams 1986, 1987, 1994; Williams *et al*. 1996). It is notable also as the source of an ejecta horizon of shocked volcanic fragments and melt material identified in late Vendian mudstone in the Adelaide fold belt ('Geosyncline' or 'Rift Complex') and Torrens Hinge Zone 240–385 km to the east and in coeval strata in the Officer Basin 540 km to the NW of Acraman (Gostin *et al*. 1986, 1989; Wallace *et al*. 1989, 1990, 1996).

The magnitude of the Acraman impact and the resulting environmental perturbations may be inferred from the properties of rocks at the strongly degraded impact site and also from the nature of the preserved ejecta horizon. Here we examine available evidence from geology, geomorphology, geochronology, geophysics and sedimentology to estimate the original size of the Acraman crater and infer the dynamics and likely environmental effects of the impact event. In doing so, we agree with Grieve (1991) that estimates of original crater dimensions should be made with caution, because processes of erosion on the Earth can enhance, modify or remove original morphological elements of an impact structure.

Geology and geomorphology of Acraman

Acraman occurs in the Gawler Range Volcanics (Fig. 1), a Mesoproterozoic continental suite of mainly acid lavas and ash flows (Blissett 1987; Fanning *et al*. 1988; Giles 1988). The flat-lying, undeformed Gawler Range Volcanics now cover $>25\,000$ km^2 and have an exposed thickness of >1 km, and outlying remnants indicate that formerly the suite was much more extensive. Acraman is underlain almost entirely by the 1592 Ma Yardea Dacite (Creaser & White 1991), the uppermost and most widespread formation of the Gawler Range Volcanics that crops out continuously over 12 000 km^2. The Yardea Dacite has an exposed thickness of 250 m but probably is much thicker, and an unknown thickness has been removed by erosion.

The Lake Acraman salina (elevation 133–138 m) is eccentrically placed within the Acraman depression (140–200 m), a near-circular low-lying area 30 km across (Figs 1 and 2). The Acraman depression marks the present extent of shattered and strongly fractured bedrock, which is more readily weathered and eroded than the undeformed rocks of the surrounding Gawler Ranges that rise up to 450 m above the lake bed. A Cretaceous high-level summit surface of the ranges, the Nott Surface (Twidale *et al*. 1976), has been dissected to 150–250 m below summit levels. The Yardea corridor 30 km south of the Acraman depression comprises several near-linear valleys up to 3 km wide that together extend for at least 70 km roughly concentric with the southern margin of the Acraman depression (Figs 1 and 2). A fault follows the Yardea corridor for 35 km.
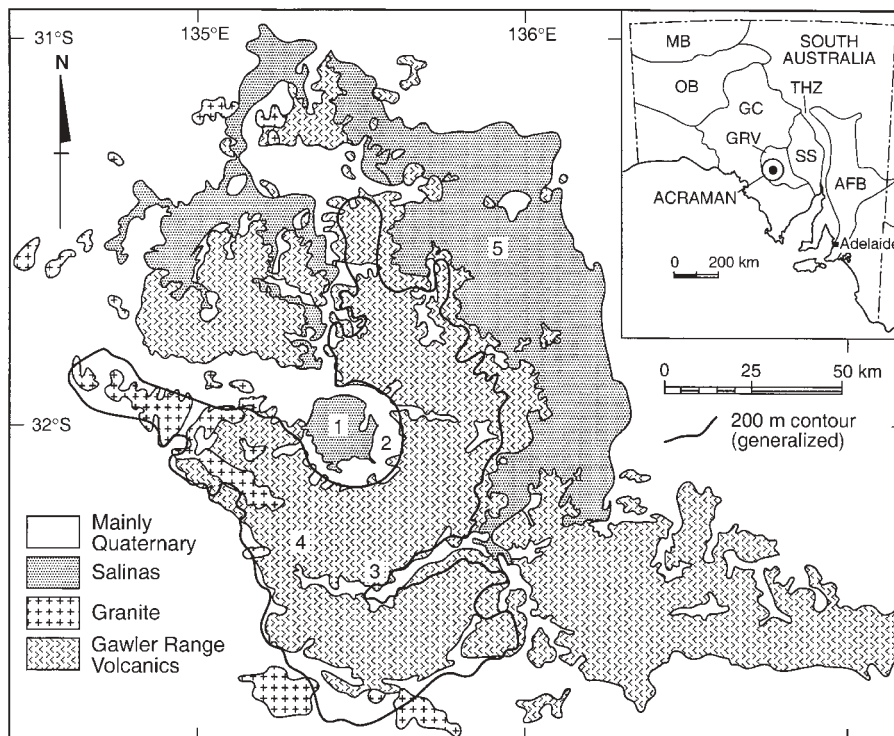
Fig. 1. Geological map of the Gawler Ranges region, South Australia, showing distribution of the 1.59 Ga Gawler Range Volcanics and coeval granites of the Hiltaba suite. 1, Lake Acraman; 2, Acraman depression; 3, Yardea corridor; 4, area of closely jointed Gawler Range Volcanics; 5, Lake Gairdner. Inset: AFB, Adelaide fold belt; THZ, Torrens Hinge Zone; SS, Stuart Shelf; GRV, Gawler Range Volcanics; GC, Gawler Craton; OB, Officer Basin; MB, Musgrave Block.
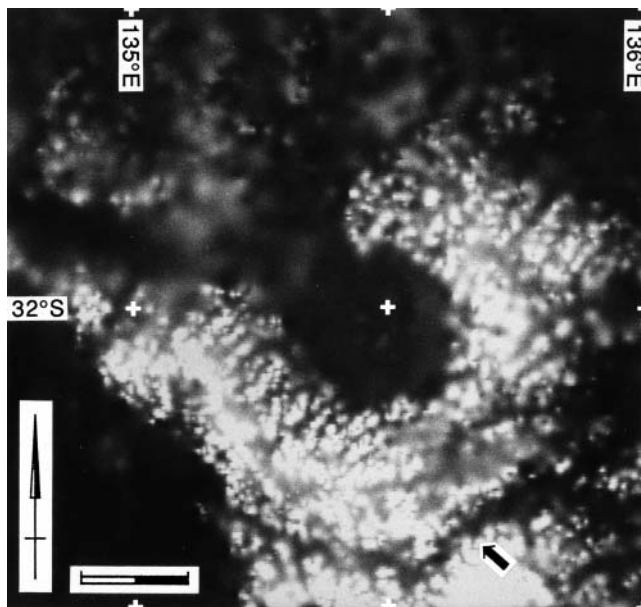

Fig. 2. Digital elevation image (greyscale: light indicates high elevations; dark indicates low elevations) of the Gawler Ranges region, showing Lake Acraman and the Acraman depression (133–200 m elevation) surrounded by an annulus of elevated country (up to 450 m), and the Yardea corridor (arrow). Scale bar represents 20 km. Image derived from data supplied by the Australian Surveying and Land Information Group (AUSLIG), Australia's national mapping agency, and reproduced by permission of the General Manager AUSLIG, Department of Administrative Services, Canberra, Australian Capital Territory.

A National Oceanographic and Atmospheric Administration (NOAA) satellite thermal IR image (Fig. 3) of Acraman shows the features at 30 and 85–90 km diameter and arcuate features at *c*. 150 km diameter.

Age of the Acraman impact

A minimum K/Ar and ^{40}Ar/^{39}Ar age for melt rock from Acraman indicates that the impact occurred at >450 Ma (Baldwin *et al*. 1991). The age of the impact is better constrained by stratigraphy. The observations listed below together argue that Acraman is the source of the ejecta horizon in mudstone near the base of the late Vendian Bunyeroo Formation in the Adelaide fold belt (Fig. 4) and Torrens Hinge Zone to the east of Acraman and in the correlative Dey Dey Mudstone (formerly Rodda beds) in the Officer Basin to the west of the impact site (Gostin *et al*. 1986, 1989; Wallace *et al*. 1989, 1990, 1996; Arouri *et al*. 2000).

(1) All large fragments (up to boulder size) and sand-grade clastic material in the ejecta were derived from felsic volcanic rocks similar to the Yardea Dacite.

(2) Comparable shattering and shock metamorphism are displayed by ejecta clasts and shattered Yardea Dacite near the centre of Acraman.

(3) A U–Pb age of 1575 ± 11 Ma for shattered euhedral zircons from ejecta clasts (Compston *et al*. 1987) is nearly concordant with the U–Pb zircon age of 1592 ± 3 Ma for the Yardea Dacite (Fanning *et al*. 1988). The slightly younger age for the ejecta may indicate derivation from a higher level than that of the dacite now exposed at the impact site, or slight displacement of the data towards the time of the impact (see Krough *et al*. 1993).

(4) The geographical distribution of the preserved ejecta horizon and the regional variation of ejecta clast size (Wallace *et al*. 1990, 1996) are consistent with Acraman as the source.

(5) Palaeomagnetic data for the Bunyeroo Formation, together with accordant palaeomagnetic data for melt rock from Acraman and modelling of the subsurface source of a magnetic anomaly at the impact site, support correlation of Acraman and the ejecta horizon in the Bunyeroo Formation (Schmidt & Williams 1991, 1996).
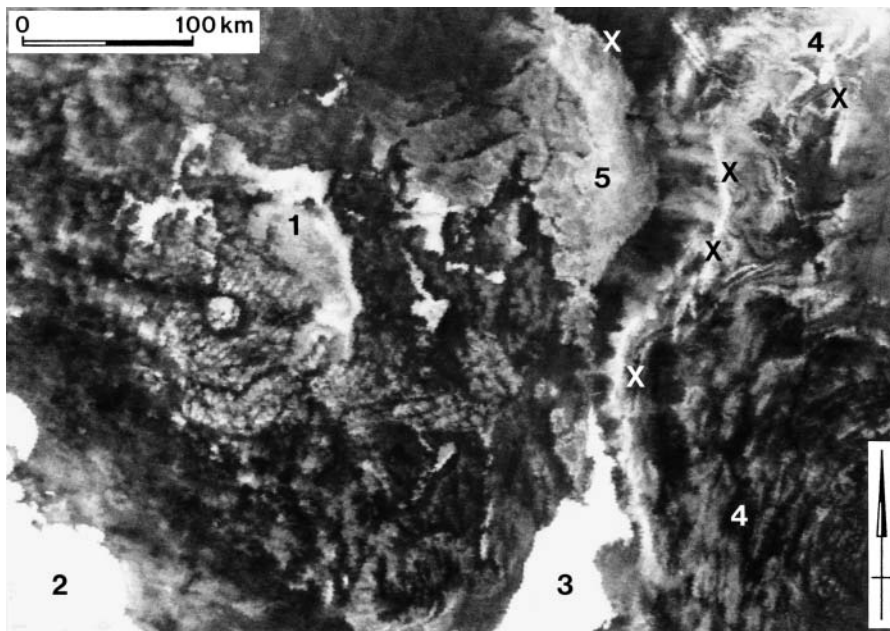
The Neoproterozoic time scale of Walter *et al*. (2000)

Fig. 3. NOAA satellite thermal IR night image of northern South Australia. 1, Lake Gairdner; 2, Great Australian Bight; 3, Spencer Gulf; 4, Flinders Ranges (Adelaide fold belt); 5, Lake Torrens. Acraman (west of Lake Gairdner) appears as a conspicuous 'bullseye' structure. The inner depression at 30 km diameter and a concentric feature at 85–90 km diameter appear cool (dark). Arcuate features at *c.* 150 km diameter comprise the southern limit of the Gawler Ranges south of Lake Acraman and a line running through Lake Gairdner. Several lineaments traverse Acraman. ×, ejecta localities in the Adelaide fold belt. NOAA9-AVHRR Band 3, Orbit no. 2246, 21 May 1985, 2200 h. Image geometrically corrected, Lambert conic conformal projection.

Fig. 4. Simplified stratigraphy of late Neoproterozoic strata in the central Adelaide fold belt and Stuart Shelf, South Australia. ▲, Sturtian and Varanger (Marinoan) glaciogenic successions. Periods (P) and Epochs (E) from Harland *et al.* (1990). ST, Sturt Tillite; HI, Holowilena Ironstone. The first signs of the Ediacara biota in South Australia appear near the top of the Wonoka Formation (Jenkins 1995).

indicates an age of *c.* 580 Ma for the Bunyeroo Formation, which may be taken as the age of the Acraman impact.

Depth of erosion since the Acraman impact

An apatite fission-track apparent age of 319 ± 19 Ma was obtained for shattered Yardea Dacite from the centre of Acraman. This age agrees with other apatite fission-track apparent ages for the Gawler Craton (mean of 13 ages is 331 ± 30 Ma; Ferguson 1981). A first-order interpretation of the apparent age is that the sample was at a temperature of 100 ± 20 °C, the apatite track retention temperature, at *c.* 320 Ma. Assuming the apparent age reflects a slow-cooling history, as suggested by the unimodal, negatively skewed distribution of the fission track lengths, the apatite track retention temperature to be 100 ± 20 °C, a mean surface palaeotemperature of 20 °C, and a normal palaeogeothermal gradient in the range $20–30$ °C km^{-1}, the apparent age would seem to require erosion of 2–5 km since 320 Ma. However, a conservative interpretation of the apatite fission-track result (Williams 1994), which allows for likely high palaeogeothermal gradients ($\geqslant 30$ °C km^{-1}) for the Gawler Craton in the late Palaeozoic, is that a maximum of *c.* 2 km of erosion has occurred near the centre of Acraman since 320 Ma.

The estimated rate of erosion in the Gawler Ranges over the past 100 million years may provide a guide to the erosion since the Acraman impact. The high-level Cretaceous Nott Surface, now dissected to depths of 250 m, is an etch surface probably once mantled by a thick regolith (Campbell & Twidale 1991). Hence, as much as 450 m of erosion may have occurred in parts of the Gawler Ranges region over the past 100 million years. The implied erosion rate of 4.5 m Ma^{-1} is of the same order as other estimates of post-Palaeozoic mean erosion rates in southeastern Australia (Lambeck & Stephenson 1986). Taking a mean rate of erosion of 4.5 m Ma^{-1} for the Gawler Ranges during the Phanerozoic suggests that *c.* 2.5 km of erosion has occurred since the Acraman impact. This figure may be a minimum because the

Gawler Craton probably was eroded severely during Permian continental glaciation (see Crowell & Frakes 1971).

Apatite fission-track data and geomorphological evidence therefore suggest that ⩾2.5 km of erosion has occurred at Acraman since the impact in the late Vendian.

Original crater dimensions

Geological evidence from Acraman

Transient cavity. Outcrop near the centre of the Acraman depression is intensely brecciated and exhibits shatter cones and planar shock-lamellae in quartz grains that indicate shock pressures of up to 15 GPa (Fig. 5). Such shock effects are confined to the centre of a complex impact structure and attenuate radially and with depth (Grieve & Pilkington 1996). Hence, before erosion, higher shock pressures would have been recorded by rocks at the centre of Acraman. Indeed, small dykes of melt rock in the central area (Williams 1994) imply that shock pressures elsewhere exceeded 70 GPa (see Melosh 1989, p. 44). The paucity of outcrop in the Acraman depression indicates that the bedrock beneath the depression is strongly disrupted by brecciation and jointing. Moreover, the exposed bedrock of the Gawler Ranges shows no evidence of faults bordering the depression. These observations and the lack of bordering faults suggest that the diameter of the Acraman depression provides a minimum estimate of the extent of the transient cavity (excavated area) and that faults marking the final structural rim occur at a greater diameter.

As noted by Grieve (1988), erosion will reduce the surface expression of the original excavated area of a degraded impact structure. He concluded that the original diameter of the excavated area at the 368 Ma Siljan impact structure in Sweden was 13–18% larger than the estimated present diameter of 22–30 km for a depth of erosion of 1.5–2 km. The implied mean erosion rate of 4.1–5.4 m Ma^{-1} is similar to that at Acraman over the past 100 million years. Moreover, Siljan and Acraman experienced glacial erosion during the Quaternary and the Permian, respectively. Assuming comparable mean rates of post-impact erosion for both regions suggests that the diameter of the

excavated area and transient cavity at Acraman was 35–40 km, up to *c.* 30% greater than the extent of the Acraman depression.

Final collapse crater. Shatter cones are initiated most frequently in rocks that experience shock pressures of 2–6 GPa, and planar shock-lamellae in quartz occur over a pressure range of 5–10 GPa to *c.* 35 GPa (Grieve & Pilkington 1996). These features show marked radial attenuation, and shock pressures of ⩽1 GPa are generally accepted as marking the limit of the transient cavity in both simple and complex impact structures (Grieve & Head 1983). Hence, obvious shock effects would not be expected in the bedrock outcrop surrounding the Acraman depression, if the limits of the depression approximate those of the transient cavity. This conclusion argues against the suggestion of Shoemaker & Shoemaker (1996) that the final collapse crater at Acraman was unlikely to have been much larger than the 30 km diameter Acraman depression because they did not observe shock effects in bedrock outside the depression. The final structural rim may be marked by the Yardea corridor at 85–90 km diameter, which is partly fault-controlled and runs close to areas of strongly fractured Yardea Dacite in the west (Fig. 1). The rectilinear form of the Yardea corridor suggests that any final collapse occurred along pre-existing fault lines.

According to Grieve (1991), the diameter of obvious excavation of a terrestrial impact structure $D_e = 0.50$–$0.65 D_f$, where D_f is the final crater diameter for crystalline targets. Lakomy (1990) gave the transient cavity diameter $D_t = (0.57 \pm 0.03) D_f$ for seven Phanerozoic impact structures. Estimated diameters of the transient cavity and final crater for the Palaeoproterozoic (*c.* 2 Ga) Vredefort impact structure in South Africa (136–152 km and 300 km), which take into account ⩾6 km of erosion, are in the ratio of 0.45–0.51 (Therriault *et al.* 1997). Diameters of the transient cavity and final crater estimated for Acraman (40 km and 85–90 km) are in the ratio of 0.44–0.47, consistent with findings for Vredefort.

Geophysical signature of Acraman

Gravity. Most topographic features within the Gawler Ranges cannot be related to the Bouguer gravity signature. The notable exception is the Acraman depression, which is marked by a near-circular negative gravity anomaly of *c.* 6 mGal that is *c.* 30 km across within a broader gravity low of *c.* 10–15 mGal amplitude and *c.* 50–60 km diameter (Fig. 6).

Near-circular negative gravity anomalies commonly are associated with impact structures (Pilkington & Grieve 1992; Grieve & Pilkington 1996), reflecting fractured and brecciated material of lower density than the surrounding undisturbed rocks. Given the strong degradation of Acraman, the magnitude of the gravity low is consistent with it marking a major impact structure with an inner area of disturbed rocks >30 km in diameter.

Aeromagnetics. High-resolution digital aeromagnetic data show that Acraman is marked by a circular magnetic low *c.* 20 km in diameter that displays subdued magnetic relief and a near-central high-amplitude (*c.* +300/−500 nT) dipolar anomaly (Fig. 7; Schmidt & Williams 1996; Williams *et al.* 1996).

According to Pilkington & Grieve (1992), the most common magnetic signature associated with impact structures is a magnetic low with subdued magnetic relief. They suggested that the diminished magnetic fields observed over craters in Precambrian crystalline terrains are due primarily to a decrease in magnetic susceptibility, and also noted that a shock-induced reduction in magnetic susceptibility occurs at shock pressures >10 GPa. The
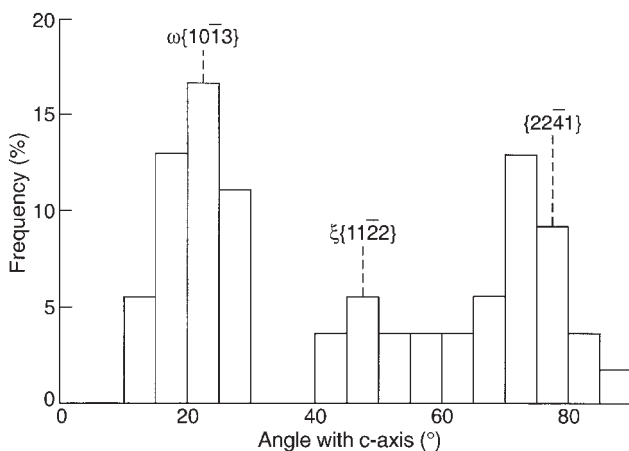

Fig. 5. Frequency histogram for the angle (in degrees) between the *c*-axis and the poles of 54 sets of planar shock-lamellae in quartz grains from shattered Yardea Dacite, central Acraman. Crystallographic orientations shown are typical of Type C shock deformation (shock pressures *c.* 15 GPa; Robertson & Grieve 1977).
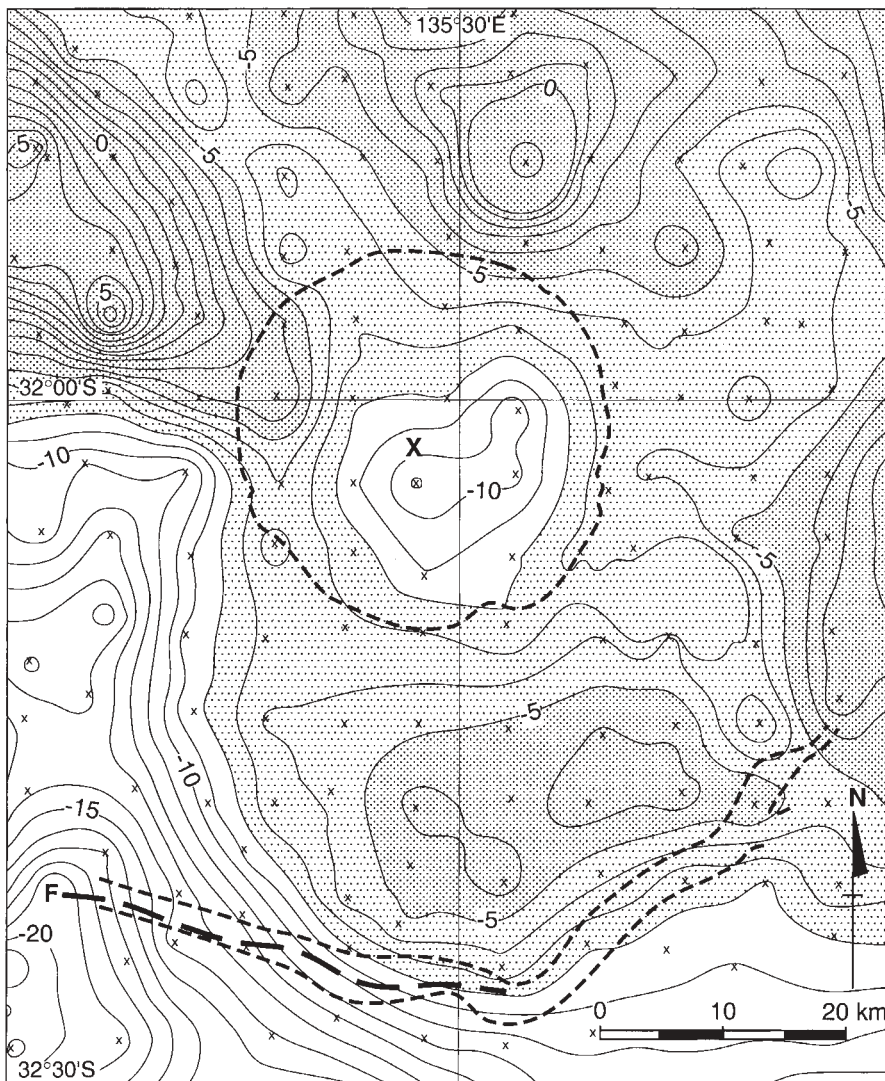
Fig. 6. Bouguer gravity anomaly map of the Gawler Ranges region, showing a negative anomaly within the Acraman depression (circular area outlined by dashed line). The Yardea corridor occurs in the south (marked by short dashes, F indicates fault). Contour interval 1 mGal. Unshaded areas indicate gravity lows; darker shading represents gravity highs. ×, gravity stations. The large cross marks the position of the near-central high-amplitude dipolar magnetic anomaly (Fig. 7). Recontoured from data of the South Australian Department of Mines and Energy, Adelaide.

magnetic susceptibility of undisturbed Yardea Dacite from the Gawler Ranges ($750–1200$ SI $\times 10^{-5}$; Zhiqun Shi 1993) is about three times greater than that of disturbed dacite from the centre of Acraman. These observations suggest that the circular magnetic low with subdued magnetic relief at Acraman largely reflects a decrease in magnetic susceptibility of bedrock over a diameter of $c.$ 20 km as a result of high shock pressures (>10 GPa).

Importantly, the diameter of the circular magnetic low would be smaller than that of the transient cavity, the limit of which is marked by shock pressures of $\leqslant 1$ GPa (see Grieve & Head 1983). The circular magnetic low may mark the extent of highly disturbed rocks of the central uplift at the present level of erosion. The near-central high-amplitude dipolar magnetic anomaly may indicate a concentration of impact melt material at shallow depth (Schmidt & Williams 1996).

Radial distance v. thickness relationship for the Acraman ejecta horizon

The main localities of the Acraman ejecta horizon are shown in Figure 8 and sections typical of the ejecta horizon in Figure 9. The horizon largely comprises angular, well-sorted, fine- to very coarse-grained, clast-supported sandstone (Wallace *et al*. 1996).

At some localities the horizon shows normal grading and was deposited by suspension settling, and at other localities it shows evidence of reworking by impact-induced tsunami (Wallace *et al*. 1996). The anomalous platinum group element geochemistry of the ejecta horizon suggests that the impactor was an asteroid (Gostin *et al*. 1989; Wallace *et al*. 1990).

Table 1 lists data for thickness of the ejecta horizon and radial distance from the centre of Acraman. The thickness data occur in four categories: (1) single measurements for primary (not reworked) sections; (2) mean values for primary sections; (3) single measurements for reworked sections; (4) mean values for reworked sections. The ejecta horizon shows variation in thickness locally, and mean values were calculated for sections measured at 10 cm intervals along a continuous outcrop several metres in extent; such thickness data include several zero values. A mean value for a locality is more representative of true thickness than is a single measurement, and reworked sections are more variable in thickness than primary sections. Hence, mean values for primary sections are the best estimates of ejecta thickness.

The ejecta horizon has been deeply buried, and the thickness measurements must be corrected for compaction to obtain original thicknesses. Compaction in sands proceeds by eliminating porosity by mechanical and chemical processes, and then by
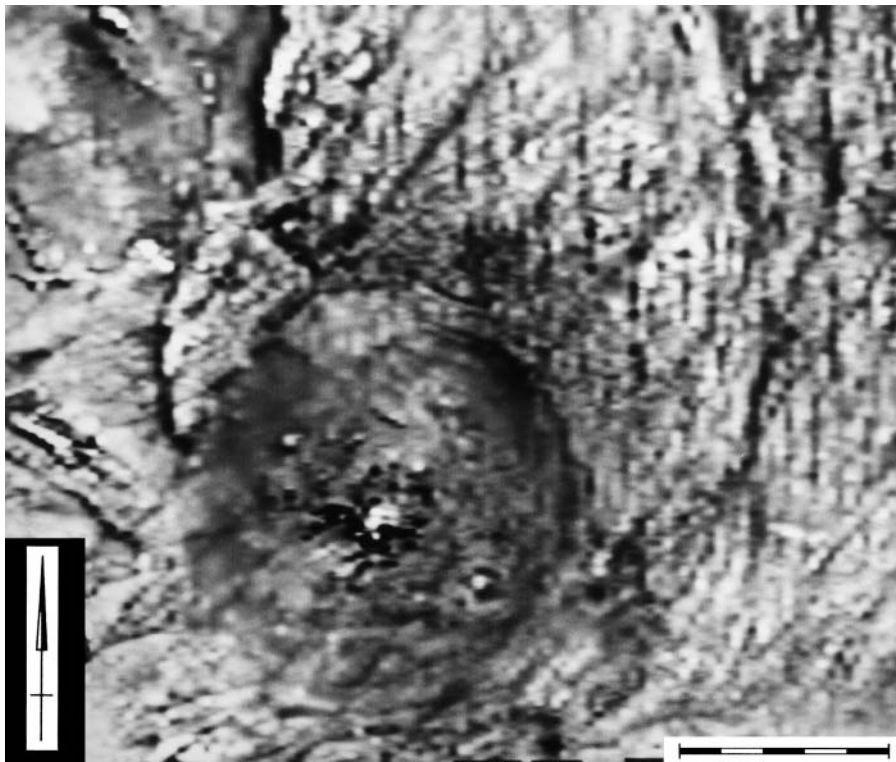
Fig. 7. Aeromagnetic image of the central part of Acraman, showing a circular magnetic low c. 20 km in diameter (dark area) that displays subdued magnetic relief, and a near-central high-amplitude dipolar anomaly (amplitude c. +300/−500 nT; white area is magnetic high). Line-spacing is 400 m along northings and eastings, with 80 m ground clearance. Earth Resources Mapper file: total magnetic intensity, greyscale, edges sharpen11. Scale bar represents 10 km. Data provided by Primary Industries and Resources South Australia, Adelaide. It should be noted that editorial staff of the *AGSO Journal of Australian Geology and Geophysics* inadvertently placed incorrect scale bars on two aeromagnetic images of Williams *et al.* (1996, figs 7 and 8), making the circular magnetic low at Acraman appear 15% smaller than its true diameter; the correct scale bar is shown here.

pressure dissolution. Well-rounded sand ranges from c. 25% to 40% porosity at deposition, the value depending on grain packing (Mitra & Beard 1980). Initial porosity in well-sorted sand also is dependent on grain angularity, the porosity increasing with increase in angularity (Fraser 1935). As the ejecta horizon consists of angular, well-sorted sands, an estimate of 30% initial porosity is probably conservative. The principal controls on sandstone compaction are burial depth, time and temperature. Given that the ejecta in the Adelaide fold belt was subjected to great burial depths (up to c. 10 km) beneath late Vendian and Cambrian strata for several tens of millions of years before Delamerian folding in the Ordovician (Preiss 1987), much vertical compaction (vertical shortening) is to be expected. The tight grain packing and typical absence of cement in the ejecta show that porosity loss has gone to completion and hence the volume reduction will be equivalent to or exceed the initial porosity. We estimate conservatively that 30% volume reduction has occurred through vertical compaction, excluding any subsequent dissolution, and this factor is used to determine the decompacted ejecta thicknesses given in Table 1.

The distances from the centre of Acraman (Table 1) have been remeasured and some amended slightly. Distances to localities east of Acraman include corrections for east–west orogenic shortening across the Torrens Hinge Zone (2% shortening) and Adelaide fold belt (25%), as measured by curvimeter from cross-sections on the Copley and Parachilna 1:250 000 geological sheets (Coats *et al.* 1973; Reid & Preiss 1999). These corrections underestimate the actual orogenic shortening, because the east–west shortening caused by Delamerian meridional and NW–SE-trending thrusts and reverse faults in the Adelaide fold belt is unknown. The distances from the centre of Acraman to the Lake Maurice West no. 1 and Observatory Hill no. 1 drill holes in the Officer Basin, which yielded cores of Dey Dey Mudstone containing single horizons of primary? Acraman ejecta (Wallace *et al.* 1989), are corrected for an estimated 10% orogenic

shortening across NE–SW-trending folds and thrusts in the eastern Officer Basin resulting from Cambrian–Ordovician and Devonian–Carboniferous deformation (Gravestock 1990; Drexel & Preiss 1995, p. 61). In addition, core of Dey Dey Mudstone from Munta no. 1 drill hole in the Officer Basin 531 km from Acraman (Fig. 8) contains at least four discrete bands, interpreted as reworked ejecta, spanning 107.6 m of section (Arouri *et al.* 2000).

Impact ejecta deposits show a non-linear decrease in thickness with radial distance from the centre of the source crater. McGetchin *et al.* (1973) found that over a wide range of scales, from small-scale laboratory cratering experiments and nuclear and high-explosive cratering events, through terrestrial simple impact craters, to estimates for lunar complex craters, ejecta blanket thickness t decreases with distance r from the crater centre as

$$t = 0.14R^{0.74}(r/R)^{-3.0} \qquad \text{for} \quad r \geq R \qquad (1)$$

where R is the radius of the 'original crater of excavation' or transient cavity and all dimensions are in metres. The ejecta investigated by McGetchin *et al.* (1973) are surficial and thickness t is for uncompacted ejecta.

Curves for predicted ejecta thickness t v. distance r based on equation (1) for transient cavity diameters of 30 km, 40 km and 50 km are shown in Figure 10, together with plots for the four categories of ejecta-horizon decompacted thickness v. radial unfolded distance from the centre of Acraman. Figure 10 shows that distance v. thickness for the Acraman ejecta accords with a transient cavity diameter of c. 40 km.

Original dimensions from integrated evidence

Evidence from geology, geomorphology, geochronology, geophysics and sedimentology provides independent and self-consistent data concerning the original dimensions of Acraman. The
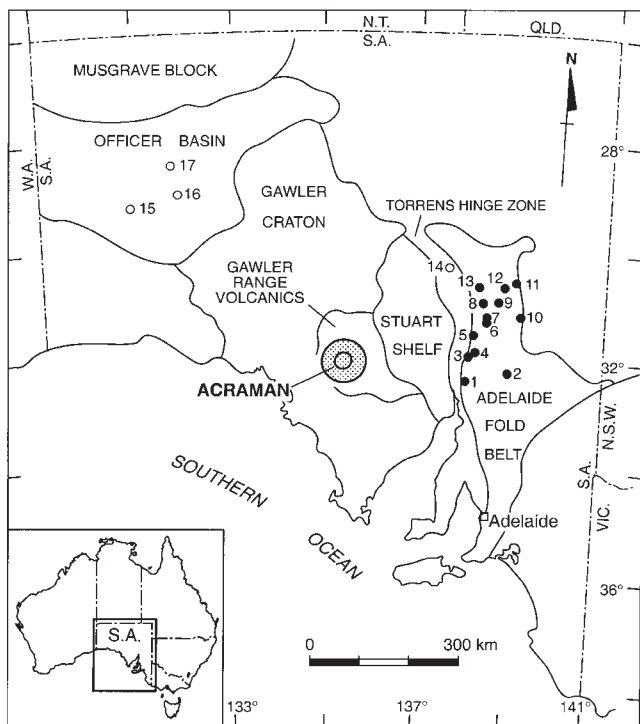
Fig. 8. Map of South Australia showing the Acraman impact site in the Mesoproterozoic Gawler Range Volcanics and ejecta occurrences in late Vendian strata of the Adelaide fold belt and Torrens Hinge Zone (Bunyeroo Formation) and Officer Basin (Dey Dey Mudstone) (see also the text, Table 1, and Figs 9 and 10). ●, ejecta seen in outcrop of the Bunyeroo Formation; ○, ejecta recorded in core from drill holes. 1, Pichi Richi Pass; 2, Bagalowie; 3, Warakimbo; 4, Yappala; 5, Merna Mora; 6, Bunyeroo Gorge; 7, Brachina Gorge; 8, Parachilna Gorge; 9, Donkey Gully; 10, Reaphook Hill; 11, Wearing Hills; 12, Jubilee Mines; 13, Trebilcock Gap; 14, Western Mining Corporation WWD no. 1; 15, Lake Maurice West no. 1; 16, Observatory Hill no. 1; 17, Munta no. 1. Ejecta localities from Gostin et al. (1986), Wallace et al. (1989, 1990) and Arouri et al. (2000), with new localities in the Adelaide fold belt from M. W. Wallace.

original crater probably comprised highly disturbed rocks of a central uplift, a transient cavity up to c. 40 km in diameter, and a possible final structural rim at 85–90 km diameter. Arcuate features at c. 150 km diameter may mark the outer limit of disturbance beyond the final structural rim. As such, Acraman ranks among the 10 largest known terrestrial impact structures (see Grieve & Shoemaker 1994). Acraman originally may have been a 'central peak crater' (see Melosh 1989, p. 133), with dimensions possibly similar to those of 'protobasins' on Mercury and Mars (Pike & Spudis 1987).

Environmental implications of the Acraman impact

The relationship between the environmental perturbations caused by impacts of asteroids and comets with the Earth and the energy of impact, as determined by Toon et al. (1997), is summarized in Table 2. For terrestrial craters >3 km diameter, the energy of impact is related to crater diameter in the expression

$$D_t = 0.64(Y/\rho_t)^{1/3.4}(v_a/v_i)^{0.1}(\cos\theta)^{0.5}(\rho_i/\rho_t)^{0.083} \quad \text{km} \quad (2)$$

where D_t is the diameter of the transient cavity, Y is the impact energy in megatons TNT (Mt), v_a is a nominal impact velocity, v_i is the actual velocity of the impactor, ρ_i is the impactor density, ρ_t is the target density, and θ is the impact angle measured from the vertical (Toon et al. 1997). Applying equation (2) to Acraman and following Toon et al. (1997) by taking $\theta = 45°$ (the most probable impact angle), $v_a = 20$ km s^{-1}, $v_i = 15$ km s^{-1} and ρ_i/ρ_t as unity, the indicated energies of impact for Acraman are as follows: $Y = 5.2 \times 10^6$ Mt for $D_t = 40$ km, $Y = 2.0 \times 10^6$ Mt for $D_t = 30$ km, and $Y = 1.1 \times 10^6$ Mt for $D_t = 25$ km.

These estimates of impact energy for Acraman exceed the nominal threshold for global catastrophe of 10^6 Mt set by Toon et al. (1997), and are much greater than the nominal thresholds of 2×10^5 Mt and 3×10^5 Mt set by Chapman & Morrison (1994) and Morrison et al. (1994), respectively. The combination of environmental perturbations given in Table 2 for impact energies $>10^6$ Mt would place great stress on the biosphere.

Palaeomagnetic data for the Bunyeroo Formation (Schmidt & Williams 1996) imply that the Acraman impact occurred at a
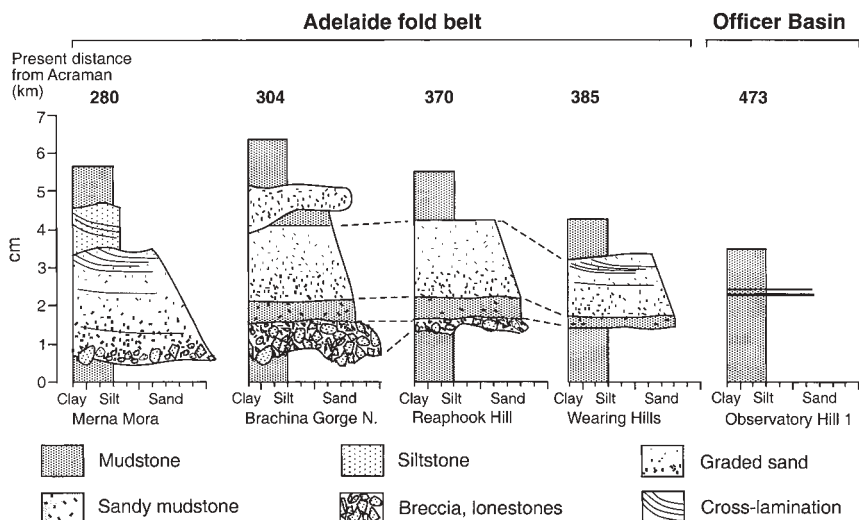

Fig. 9. Sections typical of the Acraman impact ejecta horizon in the Adelaide fold belt and Officer Basin, South Australia, arranged according to present distance from the centre of Acraman. Modified from Wallace et al. (1996).

Table 1. *Thickness of the Acraman ejecta horizon in the Adelaide fold belt, Torrens Hinge Zone and Officer Basin and radial distance from the centre of Acraman (see Fig. 8 for localities and the text for explanations of determining decompacted thickness and unfolded distance)*

Location	Sample type	Ejecta type	Measurement type	Actual ejecta thickness (mm)	Decompacted ejecta thickness (mm)	Present distance from Acraman (km)	Unfolded distance from Acraman (km)
Bagalowie	Outcrop	Primary	Single	34.8	50	323	346
Yappala	Outcrop	Primary	Single	35.4	51	277	284
Bunyeroo Gorge	Outcrop	Primary	Mean	20.4	29.1	299	305
Bunyeroo Gorge north	Outcrop	Primary	Mean	35.8	51.2	301	306
Brachina Gorge	Outcrop	Primary	Mean	37.3	53.2	304	309
Brachina Gorge north	Outcrop	Primary	Mean	26.7	38.2	304	309
Donkey Gully 1	Outcrop	Primary	Mean	35.3	50.4	332	341
Donkey Gully 2	Outcrop	Primary	Mean	28.8	41.2	332	341
Reaphook Hill	Outcrop	Primary	Mean	32.4	46.3	370	395
Jubilee Mines	Outcrop	Primary	Mean	37.2*	37.2*	359	373
Pichi Richi Pass	Outcrop	Reworked	Single	190	271	238	240
Warakimbo	Outcrop	Reworked	Single	150	214	253	256.5
Merna Mora	Outcrop	Reworked	Single	40	57	280	284
Trebilcock Gap	Outcrop	Reworked	Single	21	30	309	315
Parachilna Gorge	Outcrop	Reworked	Single	250	357	309	312
Wearing Hills	Outcrop	Reworked	Mean	17.8	25.4	385	404
WMC WWD no. 1	Drill core	Reworked	Single	25	26	277.5	278
Lake Maurice West no. 1	Drill core	Primary?	Single	7	10	541	556
Observatory Hill no. 1	Drill core	Primary?	Single	0.4	0.6	473	484

*Actual and decompacted thicknesses are the same because the ejecta horizon underwent early diagenetic cementation with carbonate.
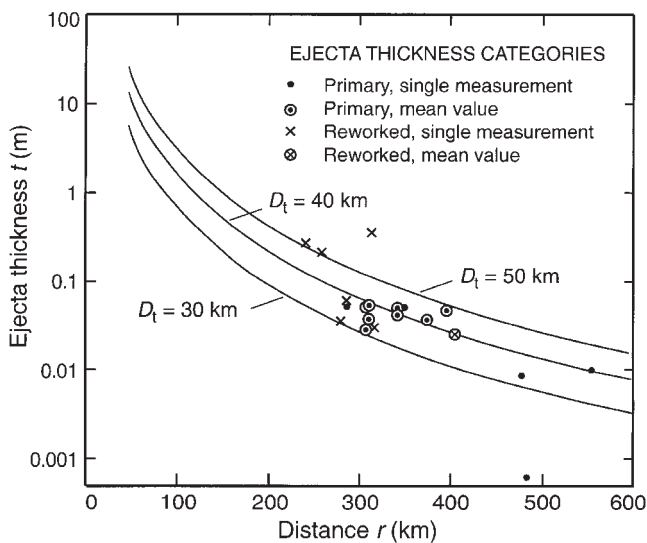

Fig. 10. Curves based on equation (1) showing predicted ejecta thickness v. distance from the centre of Acraman for transient cavity diameters D_t of 30 km, 40 km and 50 km, and points for measured thicknesses of the Acraman ejecta horizon in the Adelaide fold belt, Torrens Hinge Zone and Officer Basin (see Fig. 8 and Table 1). The Acraman ejecta thickness data are corrected for 30% vertical compaction resulting from deep burial, and are grouped in four categories. Respective distances to the centre of Acraman are corrected for orogenic shortening since the Acraman impact (see text).

of fires and atmospheric sulphate arising from the Acraman impact because of the Neoproterozoic age and volcanic target rocks, a severe perturbation of the late Vendian environment is highly probable.

This finding is consistent with evidence from the Vendian acritarch record in Australia that the Acraman impact may have induced a biotic crisis. Grey (2001) and Grey *et al*. (2003) examined the phytoplankton-diversity record for the Australian late Neoproterozoic, through biostratigraphic studies for the Adelaide fold belt, Officer Basin and Amadeus Basin. The preceding, Varanger (Marinoan) glaciation (Fig. 4), which ended at *c*. 595 Ma, does not seem to have substantially influenced the nature of the acritarch populations. Radical palynofloral change did not occur until *c*. 15 million years after the end of the Marinoan glaciation and shows a remarkable coincidence with the actual or presumed position of the Acraman ejecta horizon at *c*. 580 Ma. The palynofloral changes are marked by a rapid increase in the abundance, size and morphological complexity of planktonic acritarchs, with the first appearance of 57 species. Grey *et al*. (2003) proposed that a 'global extinction and recovery event may have been associated with the Acraman bolide impact' and speculated whether the Acraman impact may have implications for the subsequent radiation of the Metazoa.

In contrast to Acraman, two major Phanerozoic impacts that have not been linked to any known mass mortality or pulsed extinction (Chesapeake Bay and Popigai) occurred in middle and high latitudes, respectively (Poag 1997). Hence the latitude of an impact may have some influence on the ensuing environmental effects.

palaeolatitude of 12.5° + 7.1/−6.1° (Fig. 11). A major impact in low latitudes would be expected to perturb the atmosphere more widely both in the northern and southern hemispheres than would an impact of comparable magnitude in high latitudes. Hence the low latitude of the Acraman impact may have amplified the environmental effects.

We conclude that even allowing for a probable reduced level

Conclusions

The geology, geomorphology, apatite fission-track geochronology, and geophysical signature of the deeply eroded Acraman impact structure, South Australia, and the radial distance v. thickness relationship for the correlative ejecta horizon preserved in late Vendian strata, provide independent and self-consistent estimates of the original crater dimensions. The original crater

Table 2. *Environmental effects of impacts of asteroids and comets with the Earth (compiled from data of Toon* et al. *1997)*

Impact energy (Mt)	Impact frequency (years)	Environmental perturbations
c. 10^9	$>10^8$	Ocean surface waters may be acidified globally by sulphur.
$>10^7$		Blast and earthquakes cause regional damage (10^6 km²). Tsunami cresting to 100 m and flooding 20 km inland can scour the coasts of the world's oceans. Global fires. Light levels drop so low from the smoke, dust and sulphate that vision is impossible.
10^6–10^7	up to 1.5×10^7	Dust and sulphate injections cause light levels to fall below those that can support photosynthesis. Fires occur over regions $>10^7$ km², further reducing light levels.

Impact energy of 10^6 Mt is the nominal threshold for global catastrophe. Energy of the Acraman impact is 5.2×10^6 Mt for D_t *of 40 km*

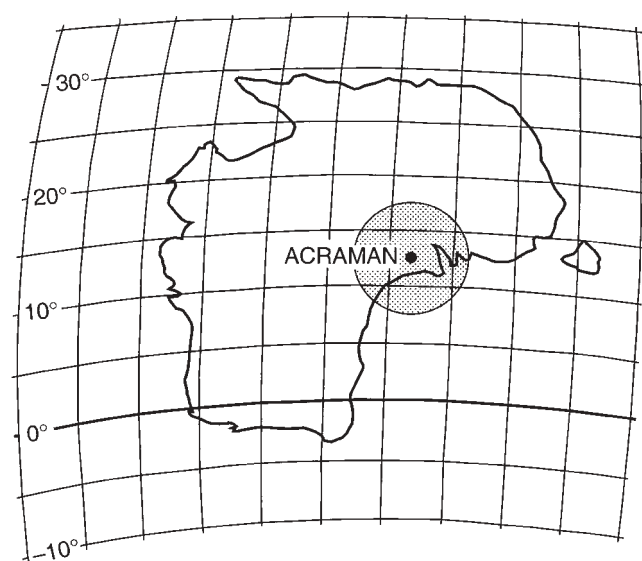|		
10^5–10^6	up to 2×10^6	Lifted dust, sulphate, and soot from fires greatly exceed those of historical volcanic eruptions. The optical effects for sulphates and dust would be comparable with those of smoke generated by a nuclear war. Ejecta plumes may produce enough NO to destroy the ozone shield.
10^4–10^5	up to 3×10^5	Stratospheric water vapour injections and ozone loss become significant globally. An energy of 10^5 Mt is a conservative lower limit at which damage may occur beyond human experience.
10^1–10^4	$<6 \times 10^4$	Blast damage, earthquakes, fires and tsunami comparable with those of natural disasters in recent history, and (excepting tsunami) confined to areas $\leqslant 10^4$–10^5 km². Tsunami could affect entire ocean basins.
$<10^1$		Negligible hazard.

Fig. 11. Palaeolatitude map of Australia in late Vendian times, based on palaeomagnetic data for the Bunyeroo Formation (Schmidt & Williams 1996). The location of Acraman and the known radial extent of the ejecta horizon (shaded circle, radius 540 km) are shown.

probably comprised highly disturbed rocks of a central uplift, a transient cavity or excavated area up to *c.* 40 km in diameter, and a possible final structural rim at 85–90 km diameter. Employing a transient cavity diameter of 40 km for Acraman gives impact energy of 5.2×10^6 Mt, which exceeds the threshold of 10^6 Mt set by Toon *et al.* (1997) for global catastrophe. The occurrence of the impact at a low palaeolatitude (*c.* 12.5°) would have permitted the atmospheric perturbations to affect both the northern and southern hemispheres.

We conclude that the Acraman impact was of sufficient magnitude to have caused a severe perturbation of the late Vendian environment. This finding supports and complements independent evidence from the Vendian acritarch record in Australia that the Acraman impact induced a biotic crisis (Grey *et al.* 2003).

References

ALVAREZ, L.W., ALVAREZ, W., ASARO, F. & MICHEL, H.V. 1980. Extraterrestrial cause for the Cretaceous–Tertiary extinction. *Science*, **208**, 1095–1108.

AROURI, K., CONAGHAN, P.J., WALTER, M.R., BISCHOFF, G.C.O. & GREY, K. 2000. Reconnaissance sedimentology and hydrocarbon biomarkers of Ediacarian microbial mats and acritarchs, lower Ungoolya Group, Officer Basin. *Precambrian Research*, **100**, 235–280.

BALDWIN, S.L., MCDOUGALL, I. & WILLIAMS, G.E. 1991. K/Ar and ⁴⁰Ar/³⁹Ar analyses of meltrock from the Acraman impact structure, Gawler Ranges, South Australia. *Australian Journal of Earth Sciences*, **38**, 291–298.

BLISSETT, A.H. (compiler) 1987. *Geological setting of the Gawler Range Volcanics*. 1:500 000 Geological Atlas Special Series, Department of Mines and Energy South Australia.

CAMPBELL, E.M. & TWIDALE, C.R. 1991. The evolution of bornhardts in silicic volcanic rocks in the Gawler Ranges. *Australian Journal of Earth Sciences*, **38**, 79–93.

CHAPMAN, C.R. & MORRISON, D. 1994. Impacts on the Earth by asteroids and comets: assessing the hazard. *Nature*, **367**, 33–40.

COATS, R.P., CALLEN, R.A. & WILLIAMS, A.F. 1973. *Copley map sheet*. 1:250 000 Geological Series, Department of Mines and Energy South Australia, Sheet **SH54-9**.

COMPSTON, W., WILLIAMS, I.S., JENKINS, R.J.F., GOSTIN, V.A. & HAINES, P.W. 1987. Zircon age evidence for the Late Precambrian Acraman ejecta blanket. *Australian Journal of Earth Sciences*, **34**, 435–445.

CREASER, R.A. & WHITE, A.J.R. 1991. Yardea Dacite—large-volume, high-temperature felsic volcanism from the Middle Proterozoic of South Australia. *Geology*, **19**, 48–51.

CROWELL, J.C. & FRAKES, L.A. 1971. Late Paleozoic glaciation: Part IV, Australia. *Geological Society of America Bulletin*, **82**, 2515–2540.

DREXEL, J.F. & PREISS, W.V. (eds) 1995. *The Geology of South Australia. Volume 2: The Phanerozoic*. Geological Survey of South Australia Bulletin **54**.

FANNING, C.M., FLINT, R.B., PARKER, A.J., LUDWIG, K.R. & BLISSETT, A.H. 1988. Refined Proterozoic evolution of the Gawler Craton, South Australia, through U–Pb zircon geochronology. *Precambrian Research*, **40/41**, 363–386.

FERGUSON, K.U. 1981. *Fission track dating of shield areas, Australia: relationships between tectonic and thermal histories and fission track age distribution*. MSc thesis, University of Melbourne.

FRASER, H.J. 1935. Experimental study of the porosity and permeability of clastic sediments. *Journal of Geology*, **43**, 910–1010.

GEHRELS, T. (ed.) 1994. *Hazards Due to Comets and Asteroids*. University of Arizona Press, Tucson.

GILES, C.W. 1988. Petrogenesis of the Proterozoic Gawler Range Volcanics, South Australia. *Precambrian Research*, **40/41**, 407–427.

GOSTIN, V.A., HAINES, P.W., JENKINS, R.J.F., COMPSTON, W. & WILLIAMS, I.S. 1986. Impact ejecta horizon within late Precambrian shales, Adelaide Geosyncline, South Australia. *Science*, **233**, 198–200.

GOSTIN, V.A., KEAYS, R.R. & WALLACE, M.W. 1989. Iridium anomaly from the Acraman impact ejecta horizon: impacts can produce sedimentary iridium peaks. *Nature*, **340**, 542–544.

GRAVESTOCK, D.I. 1990. Officer Basin petroleum potential. *In*: Parker, A.J. (compiler) *South Australia—Exploration Towards 2000*. Department of Mines and Energy South Australia, Report Book, *90/78*, 29–32.

GREY, K. 2001. Surviving the snowball Earth: the acritarch record. *In:* SIRCOMBE, K.N. & LI, Z.X. (eds) *From Basins to Mountains: Rodinia at the Turn of the Century*. Geological Society of Australia Abstracts, **65**, 45–47.

GREY, K., WALTER, M.R. & CALVER, C.R. 2003. Neoproterozoic biotic diversification: Snowball Earth or aftermath of the Acraman impact? *Geology*, **31**, 459–462.

GRIEVE, R.A.F. 1988. The formation of large impact structures and constraints on the nature of Siljan. *In:* BODEN, A. & ERIKSSON, K.G. (eds) *Deep Drilling in Crystalline Bedrock, Volume 1: The Deep Gas Drilling in the Siljan Impact Structure, Sweden, and Astroblemes*. Springer, Berlin, 328–348.

GRIEVE, R.A.F. 1991. Terrestrial impact: the record in the rocks. *Meteoritics*, **26**, 175–194.

GRIEVE, R.A.F. & HEAD, J.W. 1983. The Manicouagan impact structure: an analysis of its original dimensions and form. *Journal of Geophysical Research*, **88**(Suppl.), A807–A818.

GRIEVE, R.A.F. & PILKINGTON, M. 1996. The signature of terrestrial impacts. *AGSO (Australian Geological Survey Organisation) Journal of Australian Geology and Geophysics*, **16**, 399–420.

GRIEVE, R.A.F. & SHOEMAKER, E.M. 1994. The record of past impacts on Earth. *In:* GEHRELS, T. (ed.) *Hazards Due to Comets and Asteroids*. University of Arizona Press, Tucson, 417–462.

HARLAND, W.B., ARMSTRONG, R.L., COX, A.V., CRAIG, L.E., SMITH, A.G. & SMITH, D.G. (eds) 1990. *A Geologic Time Scale 1989*. Cambridge University Press, Cambridge.

JENKINS, R.J.F. 1995. The problems and potential of using animal fossils and trace fossils in terminal Proterozoic biostratigraphy. *Precambrian Research*, **73**, 51–69.

KOEBERL, C. & MACLEOD, K.G. (eds) 2002. *Catastrophic Events and Mass Extinctions: Impacts and Beyond*. Geological Society of America, Special Papers, **356**.

KROUGH, T.E., KAMO, S.L. & BOHOR, B.F. 1993. Fingerprinting the K/T impact site and determining the time of impact by U–Pb dating of single shocked zircons from distal ejecta. *Earth and Planetary Science Letters*, **119**, 425–429.

LAKOMY, R. 1990. Distribution of impact induced phenomena in complex terrestrial impact structures: implications for transient cavity dimensions. *In: Proceedings of the Lunar and Planetary Science Conference*. Lunar & Planetary Institute, Houston, **21**, 676–677.

LAMBECK, K. & STEPHENSON, R. 1986. The post-Palaeozoic uplift history of southeastern Australia. *Australian Journal of Earth Sciences*, **33**, 253–270.

MCGETCHIN, T.R., SETTLE, M. & HEAD, J.W. 1973. Radial thickness variation in impact crater ejecta: implications for lunar basin deposits. *Earth and Planetary Science Letters*, **20**, 226–236.

MELOSH, H.J. 1989. *Impact Cratering*. Oxford University Press, New York.

MITRA, S. & BEARD, W.C. 1980. Theoretical models of porosity reduction by pressure solution for well-sorted sandstones. *Journal of Sedimentary Petrology*, **50**, 1347–1360.

MORRISON, D., CHAPMAN, C.R. & SLOVIC, P. 1994. The impact hazard. *In:* GEHRELS, T. (ed.) *Hazards Due to Comets and Asteroids*. University of Arizona Press, Tucson, 59–91.

PIKE, R.J. & SPUDIS, P.D. 1987. Basin-ring spacing on the Moon, Mercury, and Mars. *Earth, Moon and Planets*, **39**, 129–194.

PILKINGTON, M. & GRIEVE, R.A.F. 1992. The geophysical signature of terrestrial impact structures. *Reviews of Geophysics*, **30**, 161–181.

POAG, C.W. 1997. Roadblocks on the kill curve: testing the Raup hypothesis. *Palaios*, **12**, 582–590.

PREISS, W.V. (compiler) 1987. *The Adelaide Geosyncline*. Geological Survey of South Australia Bulletin **53**.

RAUP, D.M. 1992. Large-body impact and extinction in the Phanerozoic. *Paleobiology*, **18**, 80–88.

REID, P. & PREISS, W.V. 1999. *Parachilna map sheet*. Geological Survey of South Australia Atlas 1:250 000 Series, Sheet **SH54-13**.

ROBERTSON, P.B. & GRIEVE, R.A.F. 1977. Shock attenuation at terrestrial impact structures. *In:* RODDY, D.J., PEPIN, R.O. & MERRILL, R.B. (eds) *Impact and Explosive Cratering*. Pergamon, New York, 687–702.

SCHMIDT, P.W. & WILLIAMS, G.E. 1991. Palaeomagnetic correlation of the Acraman impact structure and the Late Proterozoic Bunyeroo ejecta horizon, South Australia. *Australian Journal of Earth Sciences*, **38**, 283–289.

SCHMIDT, P.W. & WILLIAMS, G.E. 1996. Palaeomagnetism of the ejecta-bearing Bunyeroo Formation, late Neoproterozoic, Adelaide fold belt, and the age of the Acraman impact. *Earth and Planetary Science Letters*, **144**, 347–357.

SHOEMAKER, E.M. & SHOEMAKER, C.S. 1996. The Proterozoic impact record of Australia. *AGSO (Australian Geological Survey Organisation) Journal of Australian Geology and Geophysics*, **16**, 379–398.

THERRIAULT, A.M., GRIEVE, R.A.F. & REIMOLD, W.U. 1997. Original size of the Vredefort Structure: implications for the geological evolution of the Witwatersrand Basin. *Meteoritics and Planetary Science*, **32**, 71–77.

TOON, O.B., ZAHNLE, K., MORRISON, D., TURCO, R.P. & COVEY, C. 1997. Environmental perturbations caused by the impacts of asteroids and comets. *Reviews of Geophysics*, **35**, 41–78.

TWIDALE, C.R., BOURNE, J.A. & SMITH, D.M. 1976. Age and origin of palaeosurfaces on Eyre Peninsula and the southern Gawler Ranges, South Australia. *Zeitschrift für Geomorphologie*, **20**, 28–55.

WALLACE, M.W., GOSTIN, V.A. & KEAYS, R.R. 1989. Discovery of the Acraman impact ejecta blanket in the Officer Basin and its stratigraphic significance. *Australian Journal of Earth Sciences*, **36**, 585–587.

WALLACE, M.W., WILLIAMS, G.E., GOSTIN, V.A. & KEAYS, R.R. 1990. The Late Proterozoic Acraman impact—towards an understanding of impact events in the sedimentary record. *Mines and Energy Review South Australia*, **57**, 29–35.

WALLACE, M.W., GOSTIN, V.A. & KEAYS, R.R. 1996. Sedimentology of the Neoproterozoic Acraman impact-ejecta horizon, South Australia. *AGSO (Australian Geological Survey Organisation) Journal of Australian Geology and Geophysics*, **16**, 443–451.

WALTER, M.R., VEEVERS, J.J., CALVER, C.R., GORJAN, P. & HILL, A.C. 2000. Dating the 840–544 Ma Neoproterozoic interval by isotopes of strontium, carbon, and sulfur in seawater, and some interpretative models. *Precambrian Research*, **100**, 371–433.

WILLIAMS, G.E. 1986. The Acraman impact structure: source of ejecta in late Precambrian shales, South Australia. *Science*, **233**, 200–203.

WILLIAMS, G.E. 1987. The Acraman structure—Australia's largest impact scar. *Search*, **18**, 143–145.

WILLIAMS, G.E. 1994. Acraman: a major impact structure from the Neoproterozoic of Australia. *In:* DRESSLER, B.O., GRIEVE, R.A.F., & SHARPTON, V.L. (eds) *Large Meteorite Impacts and Planetary Evolution*. Geological Society of America, Special Papers, **293**, 209–224.

WILLIAMS, G.E., SCHMIDT, P.W. & BOYD, D.M. 1996. Magnetic signature and morphology of the Acraman impact structure, South Australia. *AGSO (Australian Geological Survey Organisation) Journal of Australian Geology and Geophysics*, **16**, 431–442.

ZHIQUN SHI 1993. *Automatic interpretation of potential field data applied to the study of overburden thickness and deep crustal structures, South Australia*. PhD thesis, University of Adelaide.